

# How to Evaluate Semantic Communications for Images with ViTScore Metric?

Tingting Zhu, Bo Peng, Jifan Liang, Tingchen Han, Hai Wan, Jingqiao Fu, and Junjie Chen

**Abstract**—*Semantic communications* (SC) have been expected to be a new paradigm shifting to catalyze the next generation communication, whose main concerns shift from accurate bit transmission to effective semantic information exchange in communications. However, the previous and widely-used metrics for images are not applicable to evaluate the image semantic similarity in SC. Classical metrics to measure the similarity between two images usually rely on the pixel level or the structural level, such as the PSNR and the MS-SSIM. Straightforwardly using some tailored metrics based on deep-learning methods in CV community, such as the LPIPS, is infeasible for SC. To tackle this, inspired by BERTScore in NLP community, we propose a novel metric for evaluating image semantic similarity, named *Vision Transformer Score* (ViTScore). We prove theoretically that ViTScore has 3 important properties, including *symmetry*, *boundedness*, and *normalization*, which make ViTScore convenient and intuitive for image measurement. To evaluate the performance of ViTScore, we compare ViTScore with 3 typical metrics (PSNR, MS-SSIM, and LPIPS) through 5 classes of experiments. Experimental results demonstrate that ViTScore can better evaluate the image semantic similarity than the other 3 typical metrics, which indicates that ViTScore is an effective performance metric when deployed in SC scenarios.

**Index Terms**—Image semantic similarity, pre-trained foundation model, semantic communications, semantic measurement, Vision transformer (ViT), ViTScore metric.

## I. INTRODUCTION

HIGHER bit-level precision and fewer bit-level transmission cost are the core concerns of classical transmission. Recently, a flurry of research rethinks these two major interests and investigates the concept and potential of semantics in modern and/or future communications. Shannon and Weaver (1949) once categorized communications into three levels: transmission of information symbols, semantic exchange, and effectiveness of semantic exchange [1]. This indicates that transmitting the semantics, instead of the bits or symbols, may achieve higher system efficiency. As presented in [1]–[4], *semantic communications* (SC) focus on the transmission of semantic features and the performance improvement at the semantic level, which is expected to be a new paradigm shifting to catalyze the next generation communication. SC have attracted growing interest from both academia and industry (see [4]–[22] and the references therein). However, the pioneering works on SC generally focus on the design of new schemes for SC systems. Till now, the related works

concerning the performance evaluation metric for SC are still in their infancy. Especially, the lack of desirable evaluation metrics for image semantics is highlighted. Motivated by this, we focus on the evaluation metric for image semantic similarity in this paper.

In traditional image transmission systems, the most convincing metric used to evaluate image information is based on the bit or pixel level, which encourages an exact recurrence of what has been sent from the transmitter [2]. Classical metrics of the system performance, such as *mean square error* (MSE) and *Peak Signal-to-Noise Ratio* (PSNR), usually take into account the bit (or symbol) or pixel error rate. These approaches treat each bit or pixel as equally important, which is in fact unnecessary. At the same time, they cannot describe the human perceptual judgments of images. Therefore, a class of metrics emerges to measure images at the structural level, such as the *Structural Similarity Index Metric* (SSIM) and the *Multi-Scale SSIM* (MS-SSIM). Although they are sensitive in measuring variability at the level of image luminance, contrast and structure, they are not precise in measuring image semantics. Therefore, classical metrics are not applicable to evaluate the image semantic similarity in SC.

The *artificial intelligence* (AI) technology is viewed as promising for performance improvements in complex communications scenarios that are difficult to describe with tractable mathematical models [23], [24]. Inspired by the strength of AI in semantic processing, a straightforward approach is to look for some tailored metrics based on deep-learning (DL-based) methods in *computer vision* (CV) community. However, it is infeasible for SC to directly use the DL-based metrics, such as the *Learned Perceptual Image Patch Similarity* (LPIPS)<sup>1</sup> [25]. LPIPS uses the mean pooling of feature distances from corresponding locations<sup>2</sup> to evaluate the similarity of two images. Since these features are from a bunch of convolution layers, the constraint of corresponding positions leads to the absence of global semantic measures.

We illustrate the evaluation performance of these image quality metrics with the following two typical examples. Processed by basic image transforms, *e.g.*, the gray-scale operations, an image may degrade a lot at the pixel level and the structural level, even with the DL-based metric LPIPS. However, it may still keep its semantics in significant measure. See Fig. 1 for reference. A similar phenomenon occurs in the case of image resolution processing, shown in Fig. 2.

The authors are with the School of Computer Science and Engineering and the Guangdong Key Laboratory of Information Security Technology, Sun Yat-sen University, Guangzhou 510006, China (e-mail: zhutt@mail2.sysu.edu.cn, pengb8@mail2.sysu.edu.cn, liangjf56@mail2.sysu.edu.cn, hantch@mail2.sysu.edu.cn, wanhai@mail.sysu.edu.cn, fujq3@mail.sysu.edu.cn, chenjj376@mail2.sysu.edu.cn). (Corresponding author: Hai Wan.)

<sup>1</sup>The details about the metrics (PSNR, MS-SSIM, and LPIPS) will be described in Section II.B.

<sup>2</sup>See Equation (8) for reference.

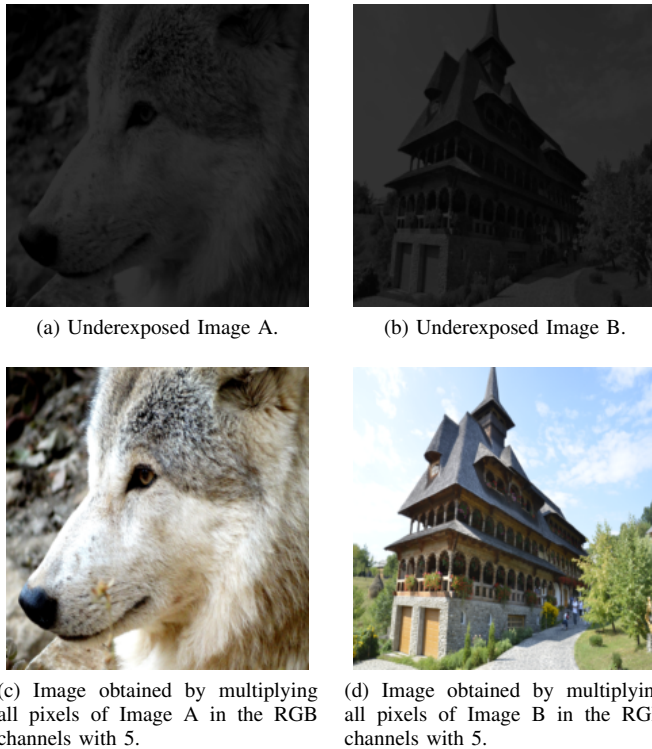


Fig. 1. Comparison of the semantic similarity between two images before and after the gray-scale operations. Here are two underexposed images (a) and (b): PSNR = 20.84, SSIM = 0.51, MS-SSIM = 0.36, LPIPS = 0.41, ViTScore<sup>4</sup> = 0.37. After transforming images, the similarity between images (c) and (d) is: PSNR = 6.59, SSIM = 0.09, MS-SSIM = 0.00, LPIPS = 0.66, ViTScore = 0.32. The fluctuation in terms of the other 4 metrics is much larger than that of ViTScore, which is almost unchanged. In fact, the semantics between these two images (a) and (c) (resp. (b) and (d)) is very similar. Hence, the semantic similarity between images (a) and (b) versus that of (c) and (d) are supposed to be close.

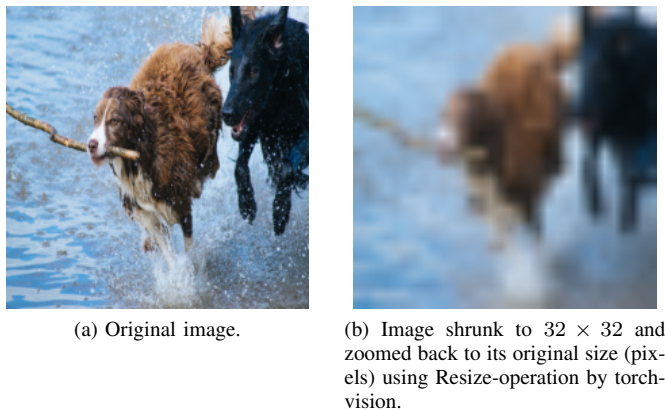


Fig. 2. Comparison of the semantic similarity between an image and its low-resolution version, which are quite semantically relevant. The similarity evaluation between images (a) and (b) is: ViTScore = 0.63, PSNR = 21.08, SSIM = 0.43, MS-SSIM = 0.74, LPIPS = 0.56.

From these two motivation examples, it is clear that a general metric for image semantic similarity is missing. Even the typical DL-based metric LPIPS cannot precisely measure the global semantics of images. To tackle this, we focus on presenting an evaluation metric that can perform well in

extracting the global semantic characters of images.

Illuminated by the advancements of textual measurement in *natural language processing* (NLP) community, we find that semantic equivalence can be evaluated automatically. Employing pre-trained contextual embedding models, the similarity of two sentences can be computed as a sum of cosine similarities between their token’s embeddings. Instead of exact matches, token similarity uses contextual embeddings. BERTScore [26], the state-of-the-art metric in the NLP community, uses max pooling of feature distances from any position. Relaxing the constraints on the corresponding locations allows the method to better capture global semantic information. Moreover, AI is undergoing a paradigm shift with the rise of foundation models [27], such as GPT-4 [28], trained on broad data at scale. Foundation models are viewed as a general paradigm of AI, which are enabled by transfer learning and scale on a technical level [27]. Within transfer learning, pre-training is a dominant approach. The basic idea of pre-training is to take the “knowledge” learned from a surrogate task and then adapt the model to the downstream task of interest via fine-tuning.

Inspired by the metric BERTScore in the NLP community and pre-training approach in foundation models, we propose a novel evaluation metric for image SC, named *Vision Transformer Score* (ViTScore), which measures the image semantic similarity based on the pre-trained image model *Vision Transformer* (ViT) [29]. ViT demonstrates a strong ability to integrate global semantic information thanks to the self-attention mechanism [29]. To the best of the authors’ knowledge, ViTScore is the first practical image semantic similarity evaluation metric based on ViT in SC. Specifically, our main contributions can be summarized as four folds:

- The ViTScore metric is first proposed to measure the semantic similarity of images based on the pre-trained model. To be specific, by exploiting the attention mechanism, a pre-trained image model ViT is employed in the ViTScore metric to learn and extract essential semantics of the image.
- We then define ViTScore (see **Definition 2**), and prove theoretically that ViTScore has 3 important properties, including symmetry, boundedness, and normalization (see **Theorems 1, 2, and 3**, respectively). These properties make ViTScore convenient and intuitive for implementation in image measurement.
- Furthermore, to evaluate the performance of ViTScore metric, we compare ViTScore with 3 typical categories of metrics (PSNR, MS-SSIM, and LPIPS) through 5 classes of experiments: (i) 7 typical image-processing case studies, (ii) universality-testing over 6 image datasets, (iii) application to CV task, (iv) evaluation in image transmission and (v) utilizing in image SC systems. Experimental evaluations show that ViTScore is robust and well-performed.
- Particularly, to verify the robustness of ViTScore for practical image processing and transmission scenarios, we utilize ViTScore by case-study of image captioning

<sup>4</sup>The details about the Vision Transformer Score (ViTScore) proposed in this paper will be described in Section III.

CV task over COCO dataset<sup>5</sup> and image transmission (concatenation of JPEG coding followed by an assuming capacity-achieving channel coding) over 6 typical datasets, respectively. In addition, we utilize ViTScore to a state-of-the-art joint source-channel coding (JSCC) scheme for image SC over the Kodak dataset. Numerical results show that ViTScore can better measure the image similarity than the other 3 typical metrics at the semantic level, indicating that ViTScore has a promising performance when deployed in SC scenarios.

The rest of this paper is structured as follows. The related works about SC for image transmission and the image semantic similarity metric are discussed in Section II. Section III introduces the proposed ViTScore metric in detail. In Section IV, the metric evaluations of ViTScore are analyzed through 5 classes of experiments. Section V draws conclusions and discusses our future work.

## II. RELATED WORK

Semantic delivery of images is essential for 6G communication systems, and hence, image SC has been studied extensively in recent years [5]. However, most of the existing research evaluates the image SC system performance with the traditional image quality metrics, which are not designed to evaluate the semantics of images. Most of the previous studies on evaluating image quality rely on the pixel level, such as  $\ell_2$  distance, MSE and PSNR. These metrics usually treat each pixel of the image as equally important, which is practically unnecessary. On the other hand, the metrics based on pixels cannot well reflect the human perceptual judgments of images. Therefore, SSIM, a class of metrics to measure images at the structural level, has emerged. There are many variants of SSIM, such as MS-SSIM, Multi-component SSIM, and Complex Wavelet SSIM. They are sensitive in demonstrating the image luminance, contrast and structure, however, they are not precise in measuring image semantics. With the prosperity of AI technology, specifically the rise of deep learning methods, some tailored DL-based metrics are developed in the CV community. Nevertheless, straightforwardly using the DL-based metrics to SC systems is infeasible. To be specific, we classify the most commonly used image quality assessment metrics into three categories.

### A. Pixel Level Measures

MSE is the simplest and most widely used image quality assessment metric. Based on MSE, the PSNR is given by

$$\text{PSNR} = 10 \log_{10} \frac{\text{MAX}^2}{\text{MSE}} (\text{dB}), \quad (1)$$

where  $\text{MSE} = d(x, \hat{x})$  is the mean square error between the reference image  $x$  and the reconstructed image  $\hat{x}$ , and MAX is the maximum possible value of the image pixels<sup>6</sup>. In general,

<sup>5</sup>The COCO dataset is a large-scale object detection, segmentation, keypoint detection, and captioning dataset. We use the image captioning part within it in this paper.

<sup>6</sup>All our experiments measured in terms of PSNR in this paper are conducted on 24-bit depth RGB images (8 bits per pixel per color channel), thus  $\text{MAX} = 2^8 - 1 = 255$ .

the larger the PSNR, the more similar the two images. PSNR is an appealing metric due to that it is simple to calculate, has clear physical meanings, and is mathematically convenient in the context of optimization. But it is not very well matched to perceived visual quality [30]–[34].

### B. Structural Level Measures

Unlike MSE and PSNR, which measure absolute error, a class of metrics focusing on human intuitive perception is presented, named SSIM. SSIM mainly considers 3 key features of an image: luminance, contrast, and structure. For two images  $A$  and  $B$ , the SSIM between them is defined as

$$\text{Luminance: } l(A, B) = \frac{2\mu_A\mu_B + c_1}{\mu_A^2 + \mu_B^2 + c_1}, \quad (2)$$

$$\text{Contrast: } c(A, B) = \frac{2\sigma_A\sigma_B + c_2}{\sigma_A^2 + \sigma_B^2 + c_2}, \quad (3)$$

$$\text{Structure: } s(A, B) = \frac{\sigma_{AB} + c_3}{\sigma_A\sigma_B + c_3}, \quad (4)$$

$$\text{SSIM: } \text{SSIM}(A, B) = [l(A, B)]^\alpha [c(A, B)]^\beta [s(A, B)]^\gamma, \quad (5)$$

where  $c_i, i \in \{1, 2, 3\}, \alpha, \beta$  and  $\gamma$  are positive constants.  $\mu$  and  $\sigma^2$  denote the mean intensity and variance of an image, respectively. Essentially, SSIM is a single-scale algorithm. The exact image scale depends on the viewing conditions of the user, such as the resolution of the display device, the viewing distance of the user, etc. Therefore, the MS-SSIM algorithm has emerged to improve evaluation performance in good agreement with human perceptual judgments. The MS-SSIM is given by

$$\text{MS-SSIM}(A, B) = [l_M(A, B)]^{\alpha M} \prod_{j=1}^M [c_j(A, B)]^{\beta_j} [s_j(A, B)]^{\gamma_j}, \quad (6)$$

where  $M$  is the maximum scale of the image. For the  $j$ -scale, the similarity in luminance, contrast and structure of  $A$  and  $B$  are denoted by  $l_j(A, B)$ ,  $c_j(A, B)$ , and  $s_j(A, B)$ , respectively. The MS-SSIM in dB is given by

$$\text{MS-SSIM} = -10 \log_{10}(1 - \text{MS-SSIM})(\text{dB}). \quad (7)$$

SSIM / MS-SSIM is between 0 and 1. Generally, the larger the SSIM / MS-SSIM, the smaller the difference between the two images at the structural level. Particularly, SSIM / MS-SSIM equals 1 if and only if the two images are exactly the same. This class of metrics well performs in measuring the image luminance, contrast and structure, but fails to evaluate for image rotation, translation, and other geometric operations.

### C. DL-based Measures

Benefiting from the deep learning methods, several DL-based metrics for image quality measurement have been developed. In [25], the authors show the unreasonable effectiveness of deep features as a perceptual metric, indicating that classification networks perform better than low-level metrics, such as  $\ell_2$ , PSNR and MS-SSIM, in evaluating the image perceptual similarity. LPIPS is the most popular one among perceptual

TABLE I  
COMPARISON OF IMAGE QUALITY METRICS WITHIN 3 TYPICAL CATEGORIES.

Categories	Metrics	Advantages	Limitations
Pixel level measures	$\ell_2$ distance, MSE, RMSE, MAE, PSNR	<ol style="list-style-type: none"> <li>1. Simple to calculate and widely used.</li> <li>2. Well perform in the MSE measurement at the pixel level.</li> <li>3. Has clear physical meanings.</li> <li>4. Mathematically convenient in the context of optimization [30].</li> </ol>	<ol style="list-style-type: none"> <li>1. Usually computed over all pixels in both images.</li> <li>2. Cannot reflect the structural and semantic information well.</li> <li>3. Poor correlation with human subjective quality ratings, unable to differentiate image contents [35].</li> <li>4. Failed to match the perceived visual quality [30].</li> </ol>
Structural level measures	SSIM [30], MSSIM [30], MS-SSIM	<ol style="list-style-type: none"> <li>1. Sensitive in measuring variability at the level of image luminance, contrast and structure.</li> <li>2. Has the properties of symmetry, boundedness, and unique maximum.</li> <li>3. Used not only to evaluate but also to optimize a large variety of signal processing algorithms and systems [36].</li> </ol>	<ol style="list-style-type: none"> <li>1. Not precise in measuring image semantics.</li> <li>2. Can not perform well with image rotation, translation, and other geometric operations.</li> </ol>
DL-based measures	LPIPS [25], VTransE [37], FID [38]	<ol style="list-style-type: none"> <li>1. Well performs in human perceptual similarity judgments.</li> <li>2. Widely used in image generation, restoration, enhancement and super-resolution.</li> </ol>	<ol style="list-style-type: none"> <li>1. Fails to precisely measure the global semantics of images.</li> <li>2. Depends on the selection of the training dataset.</li> </ol>

metrics. Given an image  $X$  and a deep neural network  $\mathcal{F}$  with  $l$  layers which takes  $X$  as its input. The output of  $i$ -th layer is denoted as  $Y_X^i \in \mathbb{R}^{H_i \times W_i \times C_i}$ , where  $H_i$ ,  $W_i$  and  $C_i$  are height, weight and number of channels of the  $i$ -th layer, respectively. Given two images  $A$  and  $B$ , the LPIPS score of them is defined as

$$\text{LPIPS}(A, B) = \sum_i \frac{1}{H_i W_i} \sum_{h,w} \|\theta^i \odot (Y_{A(h,w)}^i - Y_{B(h,w)}^i)\|_2^2 \quad (8)$$

where  $\theta^i \in \mathbb{R}^{C_i}$  are learned parameters, and  $\odot$  is the element-wise production. Typically  $\mathcal{F}$  is a pre-trained deep neural network with multiple convolution layers, and LPIPS needs to be further trained ( $\theta^i$  and/or other parameters in  $\mathcal{F}$ ). In general, the lower the LPIPS, the more similar the two images. LPIPS uses the mean pooling of feature distances from corresponding locations to evaluate the similarity of two images, leading to an absence of global semantic measures.

Table I describes the advantages and limitations of these 3 typical categories of image quality metrics in detail.

Inspired by the capacity of AI technology to process semantics, especially the advances in NLP, researchers keep a watchful eye on techniques of textual similarity metrics. Among them, the metric *bilingual evaluation understudy* (BLEU) score [39] is a widely used one to evaluate the quality of sentences that are translated by machine. The value of the BLEU score is a number ranging from 0 to 1. The higher the score, the better the quality of translation, i.e. the higher similarity between two sentences. Whereas, the BLEU score only focuses on the difference between words in two sentences rather than the semantic information similarity of two sentences. To overcome this issue, a metric, named sentence similarity, has been proposed in [40]. The metric sentence similarity is a measure closer to human judgment, defined as

$$\text{match}(\hat{\mathbf{s}}, \mathbf{s}) = \frac{\mathbf{B}_\Phi(\mathbf{s}) \cdot \mathbf{B}_\Phi(\hat{\mathbf{s}})^T}{\|\mathbf{B}_\Phi(\mathbf{s})\| \|\mathbf{B}_\Phi(\hat{\mathbf{s}})\|} \quad (9)$$

where  $\mathbf{s}$  is the transmitted sentence, and  $\hat{\mathbf{s}}$  is the reconstructed sentence,  $\mathbf{B}_\Phi$  is the *Bidirectional Encoder Representations*

*from Transformers* (BERT) based on a pre-trained language representation model with huge parameters [41]. These approaches show robust performance and achieve a higher correlation with human judgment than that of other previous metrics in many NLP tasks.

Enlightened by the boom in pre-trained models and the advantages of metrics in the NLP community, the development of semantic similarity metrics of images is encouraging. In the existing investigations of SC, only a handful of papers have studied the performance metrics, especially for images. Among the few papers that consider image transmission, most proposed SC systems are based on DL (see [37], [42]–[45] and the references therein), while none of them presents a practical semantic metric for image similarity measurement. Most existing studies on image SC systems use the PSNR, MS-SSIM or LPIPS as metrics to evaluate the performance of the system, which do not indeed evaluate the semantic information of the performance of the system. Motivated by this, we focus on developing a novel metric based on a pre-trained transformer model for the SC of images in this paper.

### III. ViTSCORE METRIC

Inspired by BERTScore [26], we propose ViTScore to evaluate the semantic similarity between two images. ViTScore uses pre-trained ViT to extract the semantic features of given images, then calculated the semantic similarity using these features. Formally, referring to [29], we give an explicit definition of ViT.

**Definition 1** (ViT). *Given an image with width of  $W$ , height of  $H$  and  $C$  channels, the ViT extracts its semantic features in an  $\frac{HW}{P^2} \times N$  matrix:*

$$\text{ViT} : \mathbb{R}^{H \times W \times C} \rightarrow \mathbb{R}^{\frac{HW}{P^2} \times N}, \quad (10)$$

where  $\mathbb{R}$  is the set of real numbers,  $P$  and  $N$  are hyperparameters of ViT. By ViT, the image is first split into multiple patches, each of which has a height of  $P$  and a width of  $P$ . Therefore the number of patches is  $\frac{HW}{P^2}$ . Then, each patch is extracted as a real vector of length  $N$ . The model overview

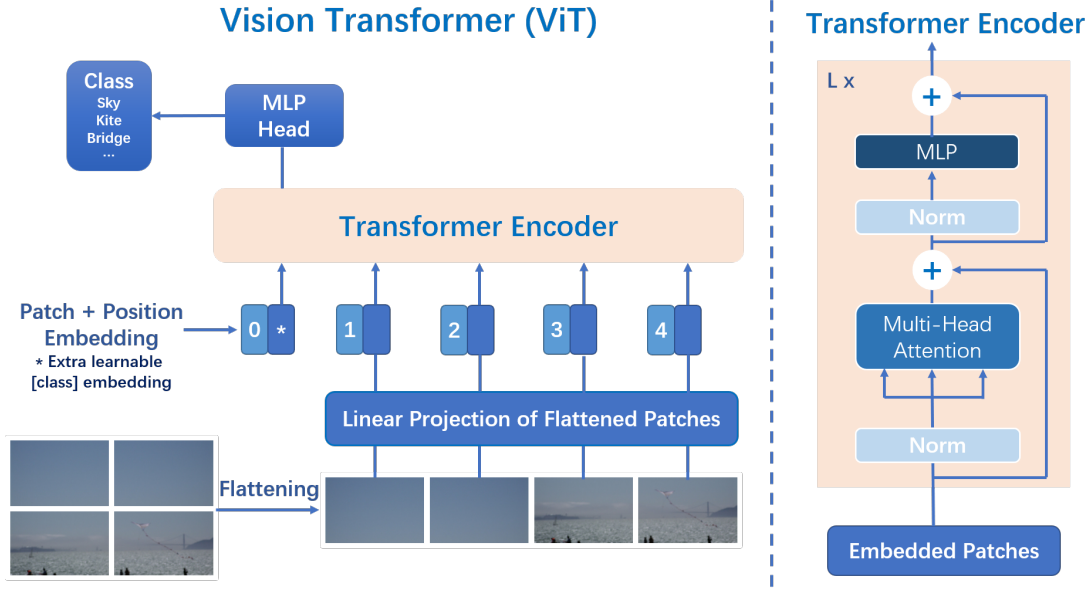


Fig. 3. The model overview of ViT [29]. The input image is first split into patches with a fixed size. Then the patches are flattened and projected to the embedding space by a linear layer. The position embedding is then added, in order to keep the positional information of patches. The mixed embedding vectors are fed into an  $L$ -layer transformer encoder. Each layer of the transformer encoder is shown on the right side of this figure. The outputs of the transformer encoder are semantic features and can be further fed into an MLP classifier. As we use ViT to extract features, our implementation does not consist of the MLP head and the classification output.

is shown in Fig. 3. Given an image  $A$  with  $n$  patches, we denote  $(\mathbf{a}_0, \mathbf{a}_1, \dots, \mathbf{a}_{n-1}) = \text{ViT}(A)$  as the semantic features extracted from ViT, where  $\mathbf{a}_i \in \mathbb{R}^N$ . The vectors are  $\ell_2$  normalized, i.e.,  $\|\mathbf{a}_i\|_2 = 1$ .

ViT is proposed as a pre-trained deep neural model for image classification. It is pre-trained with large image sets to understand the image semantics. Then it can be further fine-tuned for various downstream classification tasks. Since we use ViT to extract semantic features, we do not fine-tune ViT and use the pre-trained model parameters directly.

#### A. Definition of $\text{ViTScore}$

Based on the definition of ViT, we define  $\text{ViTScore}$  between two images as follows.

**Definition 2** ( $\text{ViTScore}$ ). Given two images:  $A$  with  $n$  patches and  $B$  with  $m$  patches. To evaluate the semantic similarity between them, we first extract their semantic features using ViT defined in Definition 1:

$$\begin{aligned} \text{ViT}(A) &= (\mathbf{a}_0, \mathbf{a}_1, \dots, \mathbf{a}_{n-1}) \\ \text{ViT}(B) &= (\mathbf{b}_0, \mathbf{b}_1, \dots, \mathbf{b}_{m-1}) \end{aligned} \quad (11)$$

Then we calculate recall  $R_{\text{ViTScore}}(A, B)$  and precision  $P_{\text{ViTScore}}(A, B)$ :

$$\begin{aligned} R_{\text{ViTScore}}(A, B) &= \frac{1}{n} \sum_{i=0}^{n-1} \max_{0 \leq j < m} \mathbf{a}_i^\top \mathbf{b}_j \\ P_{\text{ViTScore}}(A, B) &= \frac{1}{m} \sum_{j=0}^{m-1} \max_{0 \leq i < n} \mathbf{a}_i^\top \mathbf{b}_j \end{aligned} \quad (12)$$

Finally, we calculate the  $\text{ViTScore}$ :

$$\text{ViTScore}(A, B) = 2 \frac{R_{\text{ViTScore}}(A, B) \cdot P_{\text{ViTScore}}(A, B)}{R_{\text{ViTScore}}(A, B) + P_{\text{ViTScore}}(A, B)}. \quad (13)$$

#### B. Properties of $\text{ViTScore}$

$\text{ViTScore}$  has 3 important properties, including symmetry, boundedness, and normalization. We will introduce the details and provide proof in the following.

**Theorem 1** (Symmetry). For any two images  $A$  and  $B$ , changing the order of the two images does not change the  $\text{ViTScore}$ , i.e.,

$$\text{ViTScore}(A, B) = \text{ViTScore}(B, A). \quad (14)$$

*Proof.* According to Equation (12) we have

$$\begin{aligned} R_{\text{ViTScore}}(A, B) &= \frac{1}{n} \sum_{i=0}^{n-1} \max_{0 \leq j < m} \mathbf{a}_i^\top \mathbf{b}_j \\ &= P_{\text{ViTScore}}(B, A). \end{aligned} \quad (15)$$

Therefore according to Equation (13), we have

$$\begin{aligned} \text{ViTScore}(A, B) &= 2 \frac{R_{\text{ViTScore}}(A, B) \cdot P_{\text{ViTScore}}(A, B)}{R_{\text{ViTScore}}(A, B) + P_{\text{ViTScore}}(A, B)} \\ &= 2 \frac{P_{\text{ViTScore}}(B, A) \cdot R_{\text{ViTScore}}(B, A)}{P_{\text{ViTScore}}(B, A) + R_{\text{ViTScore}}(B, A)} \\ &= \text{ViTScore}(B, A). \end{aligned} \quad (16)$$

□

Since the semantic features extracted from ViT are normalized vectors,  $\mathbf{a}_i^\top \mathbf{b}_j$  is the *cosine similarity* between  $\mathbf{a}_i$  and  $\mathbf{b}_j$ .

As a result, the ViTScore shares the same boundary with cosine similarity.

**Theorem 2 (Boundedness).** *For any two images A and B, the range of ViTScore is between -1 and 1, i.e.,*

$$-1 \leq \text{ViTScore}(A, B) \leq 1. \quad (17)$$

However, we applied *greedy match* in our method, i.e., the max operator in Equation (12), the practical lower bound is higher than in Theorem 2. We will discuss the details in Section IV-A. In general, the larger the ViTScore, the more semantically similar the two images.

**Theorem 3 (Normalization).** *The ViTScore between any image A and itself is 1, i.e.,*

$$\text{ViTScore}(A, A) = 1. \quad (18)$$

*Proof.* The semantic features extracted from ViT are normalized vectors, therefore

$$\max_{0 \leq j < m} \mathbf{a}_i^\top \mathbf{a}_j = \mathbf{a}_i^\top \mathbf{a}_i = \|\mathbf{a}_i\|_2^2 = 1 \quad (19)$$

According to Equation (12), we have

$$R_{\text{ViTScore}}(A, A) = P_{\text{ViTScore}}(A, A) = 1. \quad (20)$$

Then according to Equation (13), we have

$$\text{ViTScore}(A, A) = 1. \quad (21)$$

□

Theorems 1, 2, and 3 prove that ViTScore has the important properties of symmetry, boundedness, and normalization. These important properties make ViTScore convenient and intuitive for implementation in image measurement. Table. II shows the comparison of these properties of ViTScore to the other 3 typical metrics (PSNR, MS-SSIM, and LPIPS).

TABLE II

COMPARISON OF 3 IMPORTANT PROPERTIES OF ViTSCORE TO 3 TYPICAL IMAGE METRICS.

Metrics	Symmetry	Boundedness	Normalization
ViTScore	✓	✓	✓
PSNR	✓	×	×
MS-SSIM	✓	✓	✓
LPIPS	✓	×	✓

### C. Ablation Study

An ablation study is designed to investigate whether some structure or feature of the proposed model is valid. Different metrics may have different features. For example, according to Equation (8), LPIPS uses  $\ell_2$  distance and mean pooling to evaluate the semantic similarity. While ViTScore uses cosine similarity and max pooling. To evaluate the contributions of these features, we design two *ablated* ViTScore models, named  $\text{ViTScore}_{\ell_2}$  and  $\text{ViTScore}_{\text{Mean}}$ , and compare them with the original ViTScore, named  $\text{ViTScore}_{\text{Origin}}$ , which is described in Definition 2.

First, we replace the cosine similarity in Equation (12) by  $\ell_2$  distance:

$$R_{\ell_2}(A, B) = \frac{1}{n} \sum_{i=0}^{n-1} \min_{0 \leq j < m} \|\mathbf{a}_i - \mathbf{b}_j\|_2^2, \quad (22)$$

$$P_{\ell_2}(A, B) = \frac{1}{m} \sum_{j=0}^{m-1} \min_{0 \leq i < n} \|\mathbf{a}_i - \mathbf{b}_j\|_2^2.$$

Second, we replace the max pooling in Equation (12) by mean pooling:

$$\begin{aligned} R_{\text{MeanPooling}}(A, B) &= P_{\text{MeanPooling}}(A, B) \\ &= \frac{1}{nm} \sum_{i=0}^{n-1} \sum_{j=0}^{m-1} \mathbf{a}_i^\top \mathbf{b}_j. \end{aligned} \quad (23)$$

Results are shown in Section IV-F.

## IV. ViTSCORE METRIC EVALUATION

To evaluate the performance of ViTScore for image semantic similarity, we compare ViTScore with the 3 typical categories of metrics (PSNR, MS-SSIM, and LPIPS) through 5 classes of experiments over 7 typical datasets from real-world applications and discuss the effects of the ViTScore metric. Specifically, we answer the following 5 research questions.

- *Question 1:* Does ViTScore *outperform* the previous, widely-used metrics, such as PSNR, MS-SSIM, and LPIPS, at the semantic level of images?
- *Question 2:* Is ViTScore *universal* for images semantic similarity measurement?
- *Question 3:* Is ViTScore *applicable* for practical image processing?
- *Question 4:* Is ViTScore *feasible* for practical image transmission?
- *Question 5:* How can ViTScore be *utilized in image SC* systems?

We answer the above 5 questions through 5 classes of experiments. The first one takes for example 7 typical image-processing cases to show that the proposed ViTScore evaluates semantic similarities better than 3 typical categories of metrics (PSNR, MS-SSIM, and LPIPS), consisting of an image versus its inverse, its gray-scale version, its flipping (vertical flipping and horizontal flipping), its rotation (180-degree rotation and 90-degree rotation) and versus random noise. In the second one, we study the universality of the ViTScore metric over 6 image datasets (DIV2K, Set5, Set14, B100, Urban100 and COCO), which contain both high-resolution and low-resolution images. The experimental results show that the ViTScore metric is universal and perform better than the 3 typical metrics (PSNR, MS-SSIM, and LPIPS) for the image similarity measurement in the semantic aspect. In the third one, we apply ViTScore to practical image processing with the typical image captioning CV task over the COCO dataset. And the fourth one develops ViTScore to image transmission scenarios, which indicates that ViTScore has a promising performance when deployed in SC scenarios. Particularly, we utilize ViTScore to a state-of-the-art image SC scheme, named NTSCC [13], in the last class of experiments over

the Kodak dataset. Numerical results show that ViTScore is robust when embedded in the design of image SC networks.

For fairness, we use the following experimental settings. To calculate ViTScore, we resized the input image to size  $224 \times 224 \times 3$  and fed it into the ViT model. We build upon PyTorch [46] and the timm library<sup>7</sup> [47].

All experiments are performed on a server with an Intel Xeon Gold 6248R 3.0 GHz CPU, five NVIDIA A100-PCIE-40G GPU and 128 GB of memory.

*A. Performance of Some Typical Image Processing*

We take for example 7 typical image-processing cases to show that the proposed ViTScore evaluates semantic similarities better than 3 typical categories of metrics (PSNR, MS-SSIM, and LPIPS), consisting of an image versus its inverse (obtained by 1 minus all pixels of the original image), its gray-scale version (obtained using Grayscale-operation by torch-vision), its flipping (vertical flipping and horizontal flipping), its rotation (180-degree rotation and 90-degree rotation) and versus random noise (uniformly generated in [0,1]). The overall results are shown in Fig. 4. We can find that with PSNR and MS-SSIM evaluation, the scores in most cases are similar to the random noise case, except the gray-scale case. However, with ViTScore and LPIPS evaluation, the scores in all other cases are higher than the random noise case by large margins.

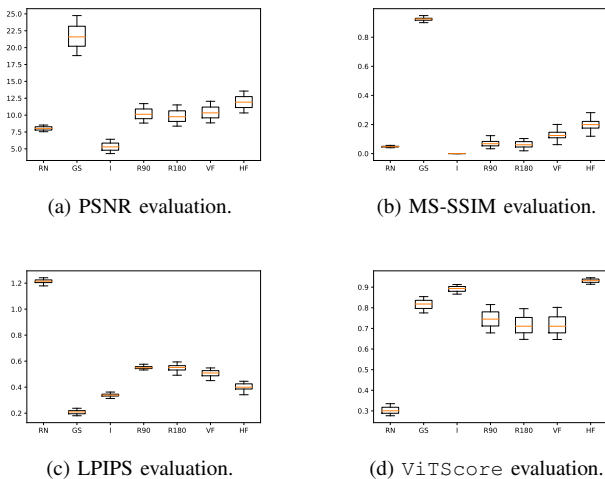


Fig. 4. The average PSNR, MS-SSIM, LPIPS and ViTScore evaluation of an image versus random noise (RN), its gray-scale version (GS), its inverse (I), its 90-degree rotation (R90), its 180-degree rotation (R180), its vertical flipping (VF), and its horizontal flipping (HF) over DIV2K dataset. Except for the gray-scale case, the PSNR and MS-SSIM evaluations in most cases are similar to the random noise case. Whereas, the LPIPS and ViTScore evaluations in all other cases are lower than the random noise case by large margins.

*(1) An image versus random noise*

First, we evaluate the ViTScore and the 3 typical metrics (PSNR, MS-SSIM, and LPIPS) between an image and some

<sup>7</sup>We use the parameters from the model vit\_base\_patch16\_224 in the timm library. By choosing appropriate parameters that are already publicly available, such as image size and patch size, we do not need to pre-train the ViT model for a specific image dataset.

random noise. As shown in Theorem 2, the theoretical lower bound of ViTScore is  $-1$ . However, it is hard to find two images that do not have any semantic similarities. Therefore, we evaluate the ViTScore between a normal image and some random noise to get a practical lower bound of our ViTScore. In our overall experiments over 6 representative image datasets (see Table III for reference), we found the minimum of ViTScore evaluation is 0.19. In this case, see Fig. 5 for reference, the PSNR between the image and random noise is 7.35, the MS-SSIM is 0.04, the LPIPS is 1.21, and the ViTScore is 0.31. We can obtain that in many other cases, the PSNR and MS-SSIM are lower than those in this case, while the images do have more semantic similarities.

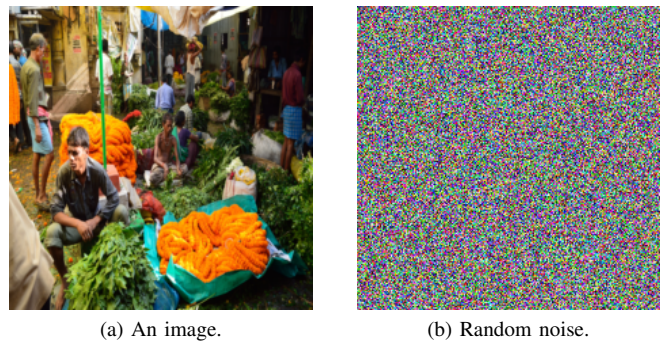


Fig. 5. An image and random noise: ViTScore = 0.31, PSNR = 7.35, MS-SSIM = 0.04, LPIPS = 1.21.

*(2) An image versus its gray-scale version*

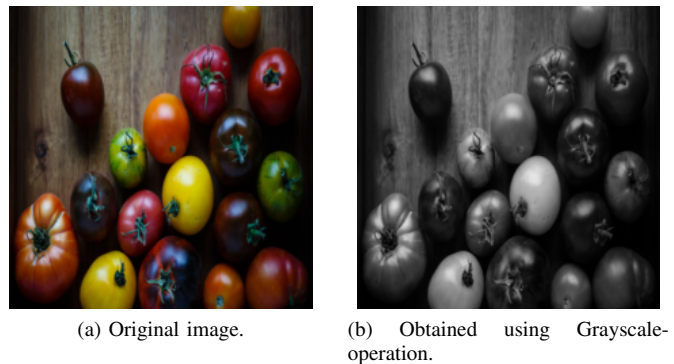


Fig. 6. An image and its gray-scale version: ViTScore = 0.81, PSNR = 18.86, MS-SSIM = 0.83, LPIPS = 0.29.

As shown in Fig. 6, converting an image to gray-scale results in a relatively high PSNR and MS-SSIM, for each pixel is modified to the average of 3 channels. The ViTScore and LPIPS evaluations show that the semantic similarity between the two images is relatively high.

*(3) An image versus its inverse*

In most cases, inverting an image barely changes its semantic information. However, while evaluating with PSNR, MS-SSIM, and LPIPS, the scores between an image and its inverse would be very low in terms of PSNR and MS-SSIM, and high in terms of LPIPS. As shown in Fig. 7, the PSNR of the two images is 5.64, the MS-SSIM is 0.00, the LPIPS is

0.39, and the ViTScore is 0.90. Compared to the gray-scale converting, which does loss semantics, the ViTScore better evaluates the semantic similarity.



(a) Original image. (b) Obtained by 1 minus all pixels of the original image.

Fig. 7. An image and its inverse: ViTScore = 0.90, PSNR = 5.64, MS-SSIM = 0.00, LPIPS = 0.39.

(4) *An image versus its rotation (180-degree rotation and 90-degree rotation)*

Rotating an image would change the position information while keeping other semantic information. As shown in Fig. 8, and Fig. 9, ViTScore gives a high score to an image and its rotation. However, the PSNR, MS-SSIM and LPIPS evaluate them at a low level.



(a) Original image. (b) Obtained by 180-degree rotation.

Fig. 8. An image and its 180-degree rotation: ViTScore = 0.71, PSNR = 8.02, MS-SSIM = 0.00, LPIPS = 0.66.



(a) Original image. (b) Obtained by 90-degree rotation.

Fig. 9. An image and its 90-degree rotation: ViTScore = 0.74, PSNR = 12.96, MS-SSIM = 0.16, LPIPS = 0.54.

(5) *An image versus its flipping (vertical and horizontal)*

In most images, such as Fig. 10, people can easily tell if an image is flipped vertically. This is presumably because of the vertical direction of gravity. On the other hand, most images like Fig. 11 are hard to tell if they are horizontally flipped. Therefore ViTScore gives a relatively low score to vertical flipping and a high score to horizontal flipping. Whereas, the PSNR, MS-SSIM and LPIPS evaluate the vertical flipping case and the horizontal flipping case both at a low level.



(a) Original image. (b) Obtained by vertical flipping.

Fig. 10. An image and its vertical flipping: ViTScore = 0.66, PSNR = 10.56, MS-SSIM = 0.00, LPIPS = 0.50.



(a) Original image. (b) Obtained by horizontal flipping.

Fig. 11. An image and its horizontal: ViTScore = 0.92, PSNR = 13.55, MS-SSIM = 0.29, LPIPS = 0.42.

In summary, the experimental results of the above 7 typical cases of image transformation in this subsection look encouraging. The results show that ViTScore has excellent performance for image semantic similarity compared with the other 3 typical metrics (PSNR, MS-SSIM, and LPIPS). Processed by basic transforms, an image may keep its semantic information by a large margin. ViTScore between the original and transformed images may stay at a high level, while the PSNR, MS-SSIM, and LPIPS between them state a considerably low level<sup>8</sup>. As the ViTScore measures the image similarity at the global semantic level, instead of the pixel or structural or local perceptual level.

B. *Universality of the ViTScore Metric*

In this experiment, we study the universality of the ViTScore metric over 6 typical image datasets (DIV2K, Set5, Set14, B100, Urban100 and COCO). Table III shows

<sup>8</sup>Recall that the higher the LPIPS score, the lower the similarity of images.

TABLE III

THE AVERAGE ViTSCORE PERFORMANCE COMPARED WITH PSNR, MS-SSIM, AND LPIPS OVER THE IMAGE DATASETS DIV2K, SET5, SET14, B100, URBAN100 AND COCO WITH 6 EXPERIMENTS. THE BEST (LOWEST IN RANDOM NOISE AND HIGHEST IN OTHERS) RESULTS ARE IN **BOLD**, AND THE SECOND-BEST RESULTS ARE WITH UNDERLINE. DEFINITIONS OF  $\bar{r}$  AND  $\bar{s}$  ARE SHOWN IN EQUATION (24).

Experiment	Metric	Dataset											
		DIV2K		Set5		Set14		B100		Urban100		COCO	
		$\bar{r}$	$\bar{s}$	$\bar{r}$	$\bar{s}$	$\bar{r}$	$\bar{s}$	$\bar{r}$	$\bar{s}$	$\bar{r}$	$\bar{s}$	$\bar{r}$	$\bar{s}$
An image versus its inverse	ViTScore	0.88	<b>6.42</b>	0.92	<b>6.61</b>	0.86	<b>7.93</b>	0.89	<b>5.61</b>	0.87	<u>4.83</u>	0.88	<b>7.15</b>
	PSNR(dB)	5.14	-2.37	4.22	-4.13	5.45	-2.09	6.01	-1.88	5.42	-2.70	5.09	-2.21
	MS-SSIM	0.00	-0.97	0.00	-1.42	0.00	-0.99	0.00	-1.03	0.00	-1.00	0.00	-0.91
	LPIPS	0.34	<u>5.04</u>	0.40	<u>4.63</u>	0.35	<u>5.74</u>	0.33	<u>5.02</u>	0.25	<b>6.45</b>	0.34	<u>6.13</u>
An image versus its 90-degree rotation	ViTScore	0.74	<b>4.74</b>	0.82	<b>5.51</b>	0.74	<b>6.21</b>	0.75	<b>4.04</b>	0.72	<b>2.97</b>	0.72	<b>5.03</b>
	PSNR(dB)	9.93	0.68	8.88	0.79	9.99	0.60	10.76	0.32	9.44	0.44	9.54	0.54
	MS-SSIM	0.07	0.27	0.07	0.88	0.04	-0.07	0.08	0.10	0.05	0.03	0.08	0.26
	LPIPS	0.55	<u>1.61</u>	0.51	<u>2.06</u>	0.56	<u>2.10</u>	0.54	<u>1.47</u>	0.57	<u>1.44</u>	0.57	<u>1.53</u>
An image versus its 180-degree rotation	ViTScore	0.72	<b>4.43</b>	0.78	<b>5.01</b>	0.72	<b>6.00</b>	0.72	<b>3.66</b>	0.72	<b>2.93</b>	0.67	<b>4.46</b>
	PSNR(dB)	9.38	0.33	9.39	1.33	9.41	0.26	10.24	0.08	9.04	0.13	8.99	0.20
	MS-SSIM	0.06	0.12	0.06	0.45	0.03	-0.21	0.07	-0.02	0.05	-0.02	0.06	0.05
	LPIPS	0.55	<u>1.61</u>	0.51	<u>2.19</u>	0.56	<u>2.13</u>	0.54	<u>1.46</u>	0.55	<u>1.70</u>	0.57	<u>1.51</u>
An image versus random noise	ViTScore	0.31	<u>-0.59</u>	0.32	-0.36	0.29	-0.01	0.31	<u>-0.92</u>	0.27	<u>-2.62</u>	0.30	-0.36
	PSNR(dB)	7.96	-0.58	7.49	<u>-0.66</u>	8.11	<u>-0.52</u>	8.34	-0.80	8.09	-0.62	7.93	<u>-0.46</u>
	MS-SSIM	0.05	-0.13	0.04	0.04	0.04	0.10	0.06	-0.21	0.05	0.05	0.05	-0.16
	LPIPS	1.21	<b>-9.43</b>	1.25	<b>-14.49</b>	1.25	<b>-9.35</b>	1.19	<b>-9.60</b>	1.21	<b>-8.66</b>	1.24	<b>-11.30</b>
An image versus its low-resolution version	ViTScore	0.63	3.30	0.77	4.91	0.63	4.69	0.63	2.68	0.59	1.34	0.61	3.64
	PSNR(dB)	20.00	<u>7.09</u>	20.34	<u>12.89</u>	19.73	<u>6.38</u>	21.61	<u>5.37</u>	17.73	<u>6.90</u>	20.74	<u>7.44</u>
	MS-SSIM	0.75	<b>12.17</b>	0.80	<b>25.61</b>	0.76	<b>17.57</b>	0.77	<b>10.16</b>	0.67	<b>13.13</b>	0.79	<b>11.47</b>
	LPIPS	0.61	0.60	0.52	1.88	0.61	1.34	0.61	0.31	0.65	0.11	0.58	1.37
An image versus its gray-scale version	ViTScore	0.81	5.54	0.88	6.15	0.84	7.71	0.83	4.94	0.86	4.70	0.82	6.32
	PSNR(dB)	19.96	7.07	17.67	<u>10.07</u>	18.59	5.71	22.51	5.79	21.15	<u>9.57</u>	20.99	7.60
	MS-SSIM	0.93	<b>15.25</b>	0.90	<b>29.00</b>	0.89	<b>20.95</b>	0.95	<b>12.75</b>	0.94	<b>18.91</b>	0.94	<b>13.81</b>
	LPIPS	0.21	<u>7.23</u>	0.22	8.61	0.20	<u>8.19</u>	0.18	<u>7.63</u>	0.12	8.46	0.17	<u>9.35</u>

the experimental results in terms of ViTScore and 3 typical categories of metrics (PSNR, MS-SSIM, and LPIPS). In this table,  $\bar{r}$  is the mean of raw scores, and  $\bar{s}$  is the mean of standard scores. Standard scores are calculated by the following equation:

$$s_{(\text{Dataset}, \text{Metric})}(r) = \text{sign}_{\text{Metric}} \frac{r - \mu_{(\text{Dataset}, \text{Metric})}}{\sigma_{(\text{Dataset}, \text{Metric})}}, \quad (24)$$

where  $\mu_{(\text{Dataset}, \text{Metric})}$  and  $\sigma_{(\text{Dataset}, \text{Metric})}$  are mean value and standard deviation of evaluation scores of any two images in the given dataset with the given metric.  $\text{sign}_{\text{Metric}} = -1$  if the metric is LPIPS (since it gives smaller scores for similar images), otherwise  $\text{sign}_{\text{Metric}} = 1$ . We can observe that the ViTScore metric is universal for image measurement over all the above-mentioned datasets. It reaches the best or the second-best performance in most experiments except the low-resolution experiment and the gray-scale experiment.

- ViTScore reaches the best performance in the 3 classes experiments (An image versus its inverse, its 90-degree rotation and its 180-degree rotation), indicating that

ViTScore is more robust in measuring the semantic similarity when the image changes in structural flipping than the other 3 metrics.

- ViTScore achieves the second-best performance on most datasets in the experiment: an image versus random noise, while LPIPS performs the best. Since the LPIPS uses the mean pooling of feature distances from corresponding locations, it fails to precisely measure the global semantics of images but is sensitive to random noise.
- In the low-resolution and gray-scale experiments, MS-SSIM performs the best. It illustrates that MS-SSIM well performs in measuring the luminance, contrast, and structure of images according to its definition. On the other hand, its standard scores are higher than the other 3 metrics' scores due to the fact the standard deviation of MS-SSIM scores of any two images in a given dataset is extremely low.

In summary, we can conclude that ViTScore outperforms the other 3 metrics (PSNR, MS-SSIM, and LPIPS) for the image similarity measurement at the global semantic level. Sur-

prisingly, ViTScore shows stable performance in the same type of experiments over all testing datasets. This suggests that ViTScore is significantly efficient in characterizing semantic aspects of images.

### C. Applications to Computer Vision Tasks

To demonstrate the performance of ViTScore when applied to practical image processing, we further employ it for downstream CV tasks. In CV field, many tasks, such as image captioning, image classification [48] and semantic segmentation [49], require a semantic understanding of an image. Therefore, we can evaluate ViTScore using these CV tasks. As our ViTScore is built from BERTScore, it is interesting to evaluate the correlation between BERTScore and ViTScore. Hence, we choose the image captioning task for an experiment in this subsection.

COCO is a representative image captioning dataset [50]. In this dataset, each image is labeled with a caption in English. The caption is able to describe the semantics of the image. Thus, we can evaluate the semantic similarities between the two images and their captions. The results are shown in Fig. 12. Based on this, we calculate the Pearson correlation coefficient (PCC) between PSNR and BERTScore, the PCC between MS-SSIM and BERTScore, the PCC between LPIPS and BERTScore, and the PCC between ViTScore and BERTScore, respectively. The PCC is defined by

$$\text{PCC}(x, y) = \frac{\text{Cov}(x, y)}{\sqrt{\text{Var}(x)\text{Var}(y)}}, \quad (25)$$

where  $\text{Cov}(\cdot)$  is the covariance function and  $\text{Var}(\cdot)$  is the variance function. Numerical results verify that ViTScore is positively correlated with BERTScore compared to PSNR, MS-SSIM, and LPIPS.

To be specific, we take for example two pairs of images to show the intuitive correlation among the 5 metrics, see Fig. 13 for reference. The first pair of images (a) and (b) in Fig. 13 has low semantic similarity. Both the BERTScore and ViTScore of them are at low levels. The second pair of images (c) and (d) in Fig. 13 has much higher semantic similarity than the first pair. Consequently, the BERTScore and ViTScore of the second one both result in a relatively high score. Whereas, the PSNR, MS-SSIM, and LPIPS seem to lose their efficacy of semantic similarity measurement in this situation.

### D. Applications to Image Transmission

In this subsection, we apply the ViTScore metric to image transmission. We use a source-channel separation-based architecture, combining JPEG source coding and an assuming capacity-achieving channel code. We carry out numerical experiments over additive white Gaussian noise (AWGN) channels to simulate real wireless image communication scenarios. The capacity of an AWGN channel is given by  $\text{Cap} = \frac{1}{2} \log_2(1 + 10^{0.1 \times \text{SNR}})$ , where SNR is the average signal-to-noise ratio  $\text{SNR} = 10 \log_{10} \frac{1}{\sigma^2}$  (dB), representing the ratio of the average power of the channel input to the average noise power. In this communication architecture, an input image is first represented as a vector of pixel intensities  $\mathbf{x} \in \mathbb{R}^n$ ,

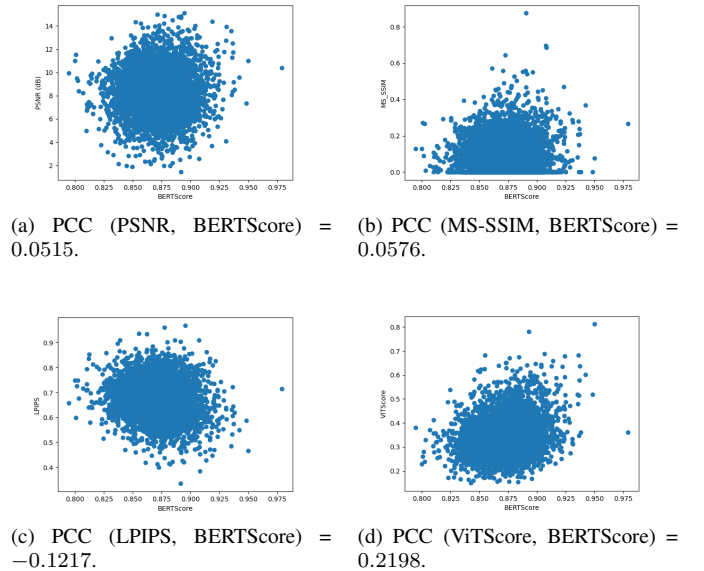


Fig. 12. The comparison of the correlations between PSNR, MS-SSIM, LPIPS, ViTScore and BERTScore over COCO dataset. The negative value of the Pearson correlation coefficient between LPIPS and BERTScore indicates higher similarity for lower LPIPS values. The Pearson correlation coefficient between ViTScore and BERTScore is larger than the absolute value of the coefficient between LPIPS and BERTScore, indicating that ViTScore is more strongly correlated with BERTScore than LPIPS.

then transmitted in  $k$  uses of an AWGN channel. The image dimension  $n$  is referred to as the *source bandwidth* and is given by the product of the image's height  $H$ , width  $W$  and the number of color channels  $C$ , i.e.,  $n = H \times W \times C$ . Utilizing JPEG coding, we define the image compression ratio as  $R_{\text{comp}} = m/n$ , where  $m$  is denoted as the size in bits of the compressed image, which is the channel input. The number of channel-use  $k$  is also defined as the *channel bandwidth*. Hence, we define the *transmission ratio* (also named as the *channel bandwidth ratio*) as  $\text{CBR} = k/n$ .

We compare the image transmission performance in terms of the average ViTScore with 3 typical metrics (PSNR, MS-SSIM, and LPIPS) over 6 image datasets. See Fig. 14, Fig. 15 and Fig. 16 for details. Experimental results show that the ViTScore is universal and robust for image transmission over all the testing image datasets. Besides, we observe that the performance trends of ViTScore are in line with those of PSNR, MS-SSIM, and LPIPS. As we have shown in the above-mentioned experiments that ViTScore outperforms the PSNR, MS-SSIM, and LPIPS for image semantic similarity, we can conclude that the proposed ViTScore metric is robust and promising when deployed in SC for images.

### E. Applications to Image Semantic Communications

In this subsection, we further analyze the application of ViTScore for image SC. In other words, we will discuss what kind of role the ViTScore could take place in image SC systems. Since we have shown the ViTScore performance in separated source-channel coding scheme in the last subsection, here we test the ViTScore performance for image SC by



(a) Image Caption in COCO dataset: A woman on a tennis court is swinging a racquet.



(b) Image Caption in COCO dataset: A painting of kids on the bathroom floor which is tile.



(c) Image Caption in COCO dataset: Beef and vegetables on a plate sitting on a table.



(d) Image Caption in COCO dataset: A white plate filled with meat and vegetables.

Fig. 13. Comparison of the evaluation examples with BERTScore, PSNR, MS-SSIM, LPIPS and ViTScore. The evaluations between (a) and (b): BERTScore = 0.89, PSNR = 16.23, MS-SSIM = 0.47, LPIPS = 0.56, ViTScore = 0.32. While the evaluations between (c) and (d): BERTScore = 0.93, PSNR = 7.28, MS-SSIM = 0.00, LPIPS = 0.61, ViTScore = 0.66. Intuitively, the semantic similarity between (c) and (d) is higher than that of (a) and (b). Surprisingly, ViTScore performs better than PSNR, MS-SSIM and LPIPS in these cases, which is consistent with BERTScore, agreeing well with human perceptual judgments.

employing a JSCC scheme. Similar to the landmark works of [13], [51]–[53], we utilized the proposed ViTScore metric to practical image SC over analog channels. To be specific, an image is first transformed into a vector of pixel intensities  $\mathbf{x} \in \mathbb{R}^n$ , then mapped to a vector of continuous-valued channel input symbols  $\mathbf{s} \in \mathbb{R}^k$  via an AI-based encoding function. The channel bandwidth ratio is defined as  $CBR = k/n$ , where  $k < n$ , denoting the code rate. Under this architecture, by introducing AI technology to extract the semantics of the image, the communication paradigm shifts to a modern version of JSCC.

We utilize the NTSCC scheme, one of the state-of-the-art image SC schemes, whose backbone is the transformer. As presented in [13], the NTSCC yields end-to-end transmission performance surpassing classical separated-based BPG source compression combined with low-density parity-check (LDPC) channel coding scheme and standard deep-JSCC methods. To compare the performance with different evaluation metrics, we take as an example the Kodak dataset, which is one of the 3 datasets used in [13]. In the considered model, the transmitter first learns a nonlinear analysis transform to map the source data into latent space, effectively extracting the source semantic features and providing side information for source-channel coding. This step is defined as semantic

encoding. Then, the encoded vectors are transmitted to the receiver via deep JSCC. The receiver reconstructs the images by synthesis transform, which can be defined as semantic decoding. The key problem of the whole NTSCC system design is an optimization problem, focusing on minimizing the rate-distortion performance of the end-to-end transmission under established perceptual quality metrics. To tackle this problem, the training loss function  $\mathcal{L}$  of the model is formulated as  $\mathcal{L} = \lambda\mathcal{L}_{CBR} + \mathcal{L}_d$ , where  $d$  is denoted as the end-to-end transmission distortion. Our main concern here is how ViTScore plays a part in this system.

A decent way is to introduce *semantic loss* to the optimization target:

$$R_{\text{sem}}(A, B) = \frac{1}{n} \sum_{i=0}^{n-1} \log \sum_{j=0}^{m-1} \exp(\mathbf{a}_i^\top \mathbf{b}_j), \quad (26)$$

$$P_{\text{sem}}(A, B) = \frac{1}{m} \sum_{j=0}^{m-1} \log \sum_{i=0}^{n-1} \exp(\mathbf{a}_i^\top \mathbf{b}_j), \quad (27)$$

$$\mathcal{L}_{\text{sem}} = 2 \frac{P_{\text{sem}}(A, B) \cdot R_{\text{sem}}(A, B)}{P_{\text{sem}}(A, B) + R_{\text{sem}}(A, B)}, \quad (28)$$

where  $A, B, n, m, \mathbf{a}_i$  and  $\mathbf{b}_j$  share the same definitions with those in Definition 2. In the training scenario,  $A$  could be the source image and  $B$  could be the target image. We can find that this equation is similar to Equation (12), by replacing the max operator with logsumexp operator. By doing so,  $\mathcal{L}_{\text{sem}}$  is smooth and can be optimized by gradient-based optimizers.

By minimizing the overall loss function  $\mathcal{L} = \mathcal{L}_{\text{ori}} + \mathcal{L}_{\text{sem}}$ , where  $\text{ori}$  is the original loss function of the SC model, we expect to enhance the semantic fidelity of the SC model. Experimental results are shown in Fig. 17 and Fig. 18.

Intuitively, the distortion performance of different systems designed based on the objective of minimizing different distortion measures varies considerably. Hence, developing a minimizing ViTScore distortion-oriented tailored system will be constructive for future work. This will help to further improve the performance of SC system solutions.

**Remark:** Fig. 17 and Fig. 18 show that the performance trends of ViTScore are in line with that of the other 3 typical metrics (PSNR, MS-SSIM, and LPIPS). That is because, in this SC scenario, the noise added in the images is additive white Gaussian noise. The semantic information between the original image and the reconstructed image varies quite a little. These metrics are consistent in their response to the effect of Gaussian noise. However, there maybe exist semantic noise in SC scenarios. Then the semantics of the image could change in the wider variation margin over transmission. The critical central character of ViTScore can play an important role in this case, for ViTScore can well evaluate the semantic similarity between the original image and the reconstructed one. It will be one of our future research directions.

#### F. Ablation Study Results

The results of the ablation study over the COCO dataset are shown in Table IV. For different forms of ViTScore have different distributions, we convert raw scores into standard

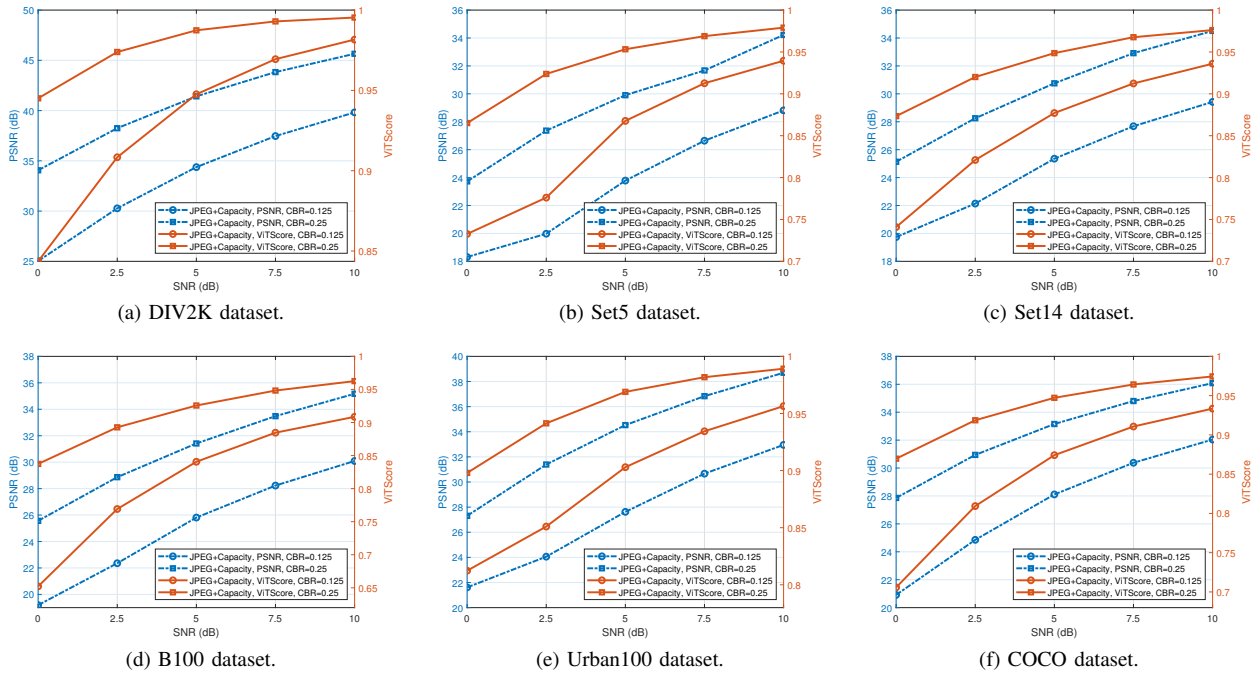


Fig. 14. The metric evaluation of the average performance of image transmission with the concatenation of JPEG code followed by an assuming capacity-achieving channel coding over an AWGN channel through 6 image datasets (DIV2K, Set5, Set14, B100, Urban100 and COCO). Average reconstruction quality increases gradually with the channel bandwidth ratio CBR increasing, as well as the channel environment improving. The performance trend of ViTScore is in line with that of PSNR over all the testing datasets.

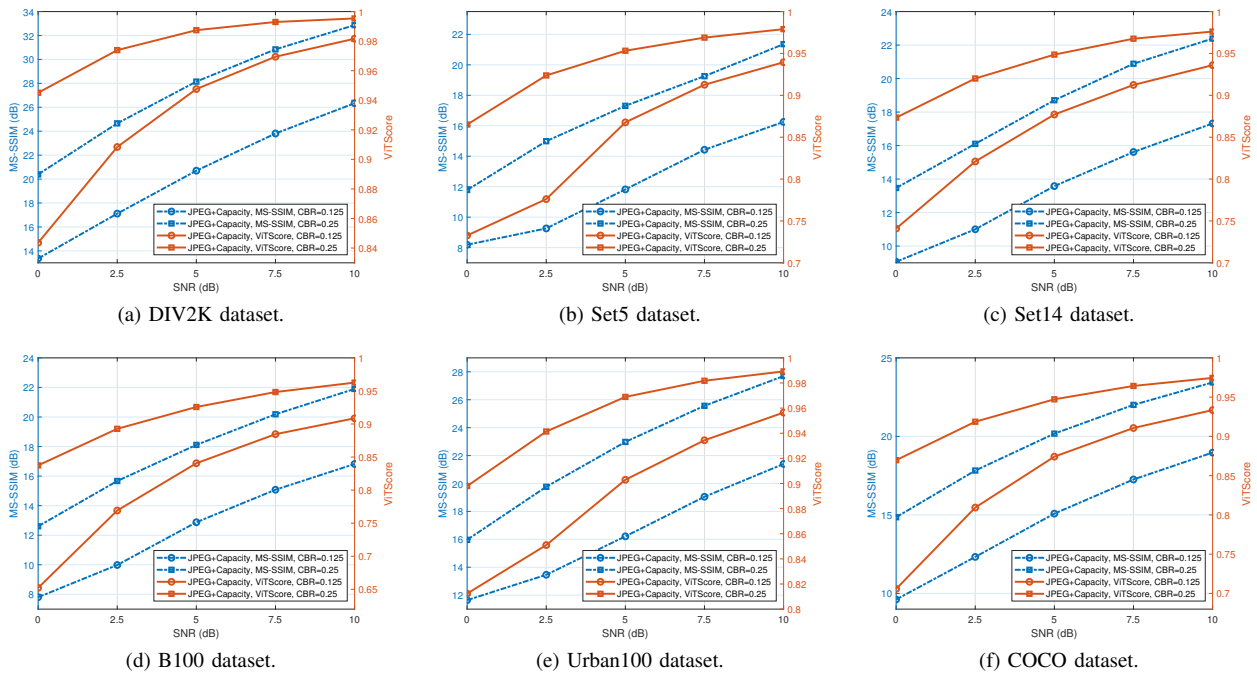


Fig. 15. The metric evaluation of the average performance of image transmission with the concatenation of JPEG code followed by an assuming capacity-achieving channel coding over an AWGN channel through 6 image datasets (DIV2K, Set5, Set14, B100, Urban100 and COCO). Average reconstruction quality increases gradually with the channel bandwidth ratio CBR increasing, as well as the channel environment improving. The performance trend of ViTScore is in line with that of MS-SSIM over all the testing datasets.

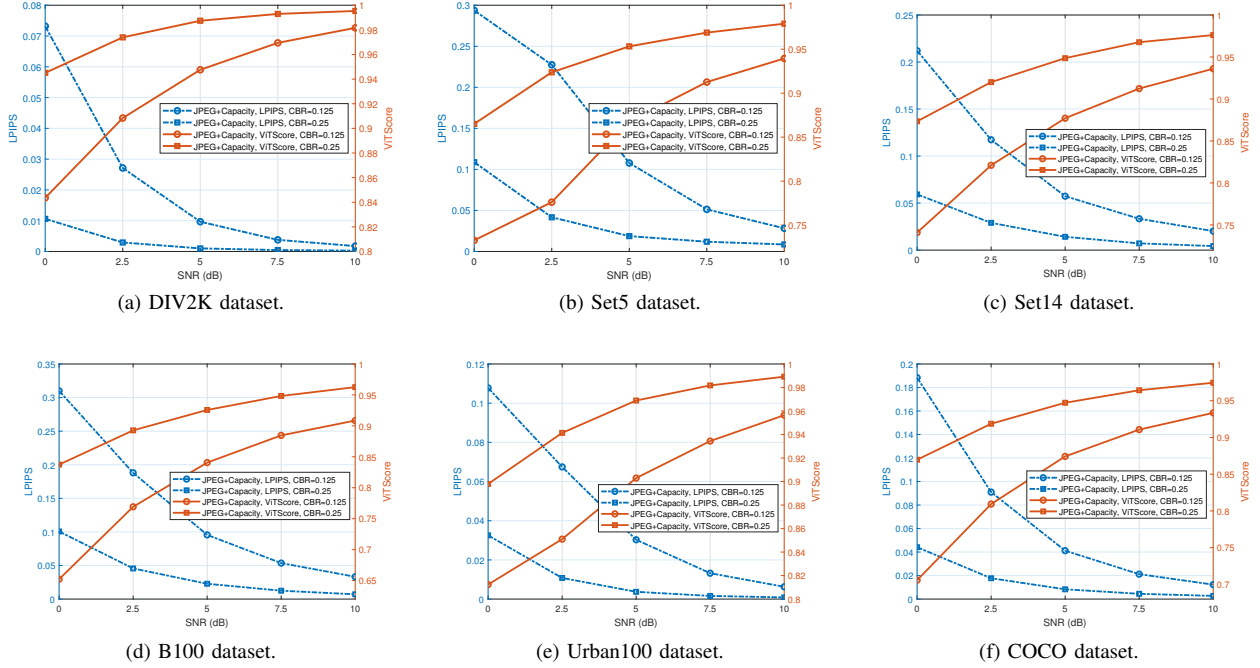


Fig. 16. The average evaluation performance of image transmission with the concatenation of JPEG code followed by an assuming capacity-achieving channel coding over an AWGN channel through 6 image datasets (DIV2K, Set5, Set14, B100, Urban100 and COCO). Average reconstruction quality increases gradually with the channel bandwidth ratio CBR increasing, as well as the channel environment improving. The performance trend of ViTScore is in line with that of the DL-based metric LPIPS over all the testing datasets. For LPIPS, the lower the better; while for ViTScore, the higher the better.

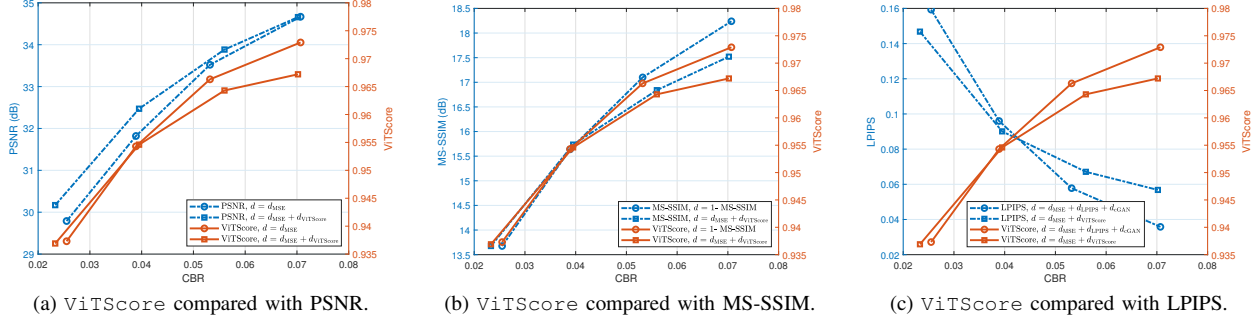


Fig. 17. The metric evaluation of the average performance of image semantic communications based on the NTSCC scheme over an AWGN channel at SNR = 10dB through the Kodak dataset. Average reconstruction quality increases gradually with the channel bandwidth ratio CBR increasing, as well as the channel environment improving. The performance trends of ViTScore are in line with those of the other 3 typical metrics (PSNR, MS-SSIM, and LPIPS).

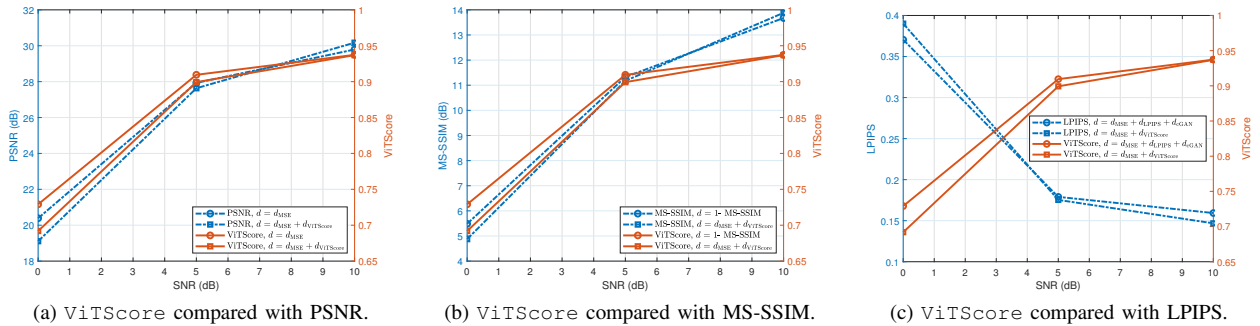


Fig. 18. The metric evaluation of the average performance of image semantic communications based on the NTSCC scheme versus the SNR at the AWGN channel through the Kodak dataset with the average channel bandwidth ratio fixed CBR  $\approx$  0.025. Average reconstruction quality increases gradually with the channel environment improving, i.e., the SNR increasing. The performance trends of ViTScore are in line with those of the other 3 typical metrics (PSNR, MS-SSIM, and LPIPS).

scores by Equation (24). We can find that, (1) compared to the  $\ell_2$  version, the original ViTScore achieves better performance in all experiments; (2) compared to the mean pooling version, the original ViTScore achieves better performance in most experiments, except in the random noise experiment. This is due to the tolerance of max pooling. Overall, the original ViTScore can better reflect the semantic similarity.

TABLE IV  
ABLATION STUDY RESULTS. RAW SCORES ARE CONVERTED INTO STANDARD SCORES. THE BEST RESULTS ARE SHOWN IN **BOLD**.

Experiment	ViTScore <sub>Origin</sub>	ViTScore <sub><math>\ell_2</math></sub>	ViTScore <sub>Mean</sub>
GS	<b>6.32</b>	6.25	4.78
I	<b>7.15</b>	7.07	5.10
R90	<b>5.03</b>	4.97	4.14
R180	<b>4.46</b>	4.40	3.66
RN	-0.36	-0.14	<b>-0.83</b>
LR	<b>3.64</b>	3.59	3.18

### G. Evaluation Summary

In this section, we have evaluated the ViTScore metric performance through 5 classes of experiments. We report results on downstream datasets in terms of 3 typical categories of metrics (PSNR, MS-SSIM, and LPIPS) and ViTScore. Overall, merits of ViTScore include:

- compared with the other 3 typical metrics, ViTScore shows its robustness for image semantic similarity measurement;
- over all the testing datasets, ViTScore shows its universality in image semantic measurement;
- applied to downstream CV task, ViTScore shows its potential in image captioning task, well reflecting the semantic similarity;
- applied to practical image transmission scenarios, ViTScore shows its feasibility as a fidelity criterion of the communication system at the semantic level;
- utilized to the NTSCC scheme, ViTScore shows its well-performance when embedded in the design of image SC networks.

Besides, in the case of image transmission and semantic communications, the trends of the performance evaluated with the ViTScore metric are consistent with those of the other 3 typical metrics. It evidences that ViTScore is a promising alternative to existing widely used metrics for image transmission systems. In particular, ViTScore will play a crucial part in SC systems when semantic noise is added to the communication system, that is, the semantics of the transmitted image is extremely changed. Moreover, we perform an ablation study of ViTScore to show the optimal structure of ViTScore. Further analysis of ViTScore performance properties is an exciting direction for future work.

## V. CONCLUSION AND DISCUSSION

In this paper, we have proposed ViTScore, a novel semantic similarity evaluation metric for images based on

the pre-trained image model ViT. To the authors' knowledge, ViTScore is the first practical image semantic similarity metric for SC. We define the ViTScore and prove theoretically that, ViTScore has the properties of *symmetry*, *boundedness*, and *normalization*. These important properties make ViTScore convenient and intuitive for implementation in image measurement. Furthermore, we evaluate the performance of ViTScore through 5 classes of experiments over several typical image datasets. Experiment results show that ViTScore is robust and well-performed. Thanks to exploiting the attention mechanism of pre-trained models, ViTScore can automatically learn and extract essential semantics of the image. Therefore, ViTScore exhibits an excellent ability to measure the semantics of images. Particularly, we compare ViTScore with 3 typical categories of metrics (PSNR, MS-SSIM, and LPIPS) in application to practical image processing and transmission scenarios. Numerical results demonstrate that ViTScore is more efficient than the other 3 metrics for focusing on the global semantic level rather than the pixel or structural level. Accordingly, we believe that ViTScore has a promising performance in the case when deployed in SC scenarios.

Currently, this work is just a first step towards SC for images. Advances in the foundation models, such as GPT-4, and their applications in future communications can bring further performance improvements in image transmission. The metric ViTScore proposed in this paper can be easily extended along with foundation models. Furthermore, a general framework design of SC for image and video, especially combined with JSCC, will be our future work.

## VI. ACKNOWLEDGMENTS

**This research was supported by** the National Key R&D Program of China (No. 2021YFA1000500), the NSF of China (No. 61976232), the Guangdong Basic and Applied Basic Research Foundation (No. 2022A1515011355) and the Guizhou Science Support Project (No. 202201011699). **We also would like to express our sincere gratitude to Prof. Xiao Ma** for valuable discussion and constructive comments, which have greatly improved this paper.

## REFERENCES

- [1] C. E. Shannon and W. Weaver, "The mathematical theory of information," *Urbana: University of Illinois Press*, vol. 97, no. 6, pp. 128–164, 1949.
- [2] K. Lu, Q. Zhou, R. Li *et al.*, "Rethinking modern communication from semantic coding to semantic communication," *IEEE Wireless Communications*, pp. 1–13, 2022.
- [3] J. Hoydis, F. A. Aoudia, A. Valcarce, and H. Viswanathan, "Toward a 6G AI-native air interface," *IEEE Communications Magazine*, vol. 59, no. 5, pp. 76–81, 2021.
- [4] W. Tong and G. Y. Li, "Nine challenges in artificial intelligence and wireless communications for 6G," *IEEE Wireless Communications*, 2022.
- [5] D. Gündüz, Z. Qin, I. E. Aguerri *et al.*, "Beyond transmitting bits: Context, semantics, and task-oriented communications," *IEEE Journal on Selected Areas in Communications*, vol. 41, no. 1, pp. 5–41, 2022.
- [6] M. Sana and E. C. Strinati, "Learning semantics: An opportunity for effective 6G communications," in *proc. IEEE 19th Annual Consumer Communications & Networking Conference (CCNC)*, 2022, pp. 631–636.

- [7] M. K. Farshbafan, W. Saad, and M. Debbah, "Common language for goal-oriented semantic communications: A curriculum learning framework," in *proc. IEEE International Conference on Communications (ICC)*, 2022, pp. 1710–1715.
- [8] E. Beck, C. Bockelmann, and A. Dekorsy, "Semantic communication: An information bottleneck view," 2022, *arXiv:2204.13366*. [Online]. Available: <https://arxiv.org/abs/2204.13366>.
- [9] X. Kang, B. Song, J. Guo *et al.*, "Task-oriented image transmission for scene classification in unmanned aerial systems," *IEEE Transactions on Communications*, vol. 70, no. 8, pp. 5181–5192, 2022.
- [10] M. Jankowski, D. Gündüz, and K. Mikolajczyk, "Wireless image retrieval at the edge," *IEEE Journal on Selected Areas in Communications*, vol. 39, no. 1, pp. 89–100, 2021.
- [11] Q. Hu, G. Zhang, Z. Qin *et al.*, "Robust semantic communications against semantic noise," in *proc. IEEE 96th Vehicular Technology Conference (VTC)*, 2022, pp. 1–6.
- [12] K. Liu, D. Liu, L. Li *et al.*, "Semantics-to-signal scalable image compression with learned reversible representations," *International Journal of Computer Vision*, vol. 129, no. 9, pp. 2605–2621, 2021.
- [13] J. Dai, S. Wang, K. Tan *et al.*, "Nonlinear transform source-channel coding for semantic communications," *IEEE Journal on Selected Areas in Communications*, pp. 2300–2315, 2022.
- [14] E. Boursoulatte, D. B. Kurka, and D. Gündüz, "Deep joint source-channel coding for wireless image transmission," in *proc. IEEE International Conference on Acoustics, Speech and Signal Processing (ICASSP)*, 2019, pp. 4774–4778.
- [15] H. Xie, Z. Qin, G. Y. Li, and B.-H. Juang, "Deep learning enabled semantic communication systems," *IEEE Transactions on Signal Processing*, vol. 69, pp. 2663–2675, 2021.
- [16] D. Huang, X. Tao, F. Gao, and J. Lu, "Deep learning-based image semantic coding for semantic communications," in *proc. IEEE Global Communications Conference (GLOBECOM)*, 2021, pp. 1–6.
- [17] H. Xie, Z. Qin, and G. Y. Li, "Task-oriented multi-user semantic communications for VQA," *IEEE Wireless Communications Letters*, vol. 11, no. 3, pp. 553–557, 2021.
- [18] H. Xie, Z. Qin, X. Tao, and K. B. Letaief, "Task-oriented multi-user semantic communications," *IEEE Journal on Selected Areas in Communications*, pp. 1–1, 2022.
- [19] B. Güler, A. Yener, and A. Swami, "The semantic communication game," *IEEE Transactions on Cognitive Communications and Networking*, vol. 4, no. 4, pp. 787–802, 2018.
- [20] Y. Zhang, H. Zhao, J. Wei *et al.*, "Context-based semantic communication via dynamic programming," *IEEE Transactions on Cognitive Communications and Networking*, vol. 8, no. 3, pp. 1453–1467, 2022.
- [21] S. Yao, K. Niu, S. Wang, and J. Dai, "Semantic coding for text transmission: An iterative design," *IEEE Transactions on Cognitive Communications and Networking*, vol. 8, no. 4, pp. 1594–1603, 2022.
- [22] H. Seo, J. Park, M. Bennis, and M. Debbah, "Semantics-native communication via contextual reasoning," *IEEE Transactions on Cognitive Communications and Networking*, 2023.
- [23] T. O'shea and J. Hoydis, "An introduction to deep learning for the physical layer," *IEEE Transactions on Cognitive Communications and Networking*, vol. 3, no. 4, pp. 563–575, 2017.
- [24] O. Simeone, "A very brief introduction to machine learning with applications to communication systems," *IEEE Transactions on Cognitive Communications and Networking*, vol. 4, no. 4, pp. 648–664, 2018.
- [25] R. Zhang, P. Isola, A. A. Efros *et al.*, "The unreasonable effectiveness of deep features as a perceptual metric," in *Proceedings of the IEEE conference on computer vision and pattern recognition*, 2018, pp. 586–595.
- [26] T. Zhang, V. Kishore, F. Wu *et al.*, "BERTScore: Evaluating text generation with BERT," 2019, *OpenReview*. [Online]. Available: <https://openreview.net/forum?id=SkeHuCVFDr>.
- [27] R. Bommasani, D. A. Hudson, E. Adeli *et al.*, "On the opportunities and risks of foundation models," *arXiv preprint arXiv:2108.07258*, 2021.
- [28] OpenAI, "GPT-4 technical report," 2023, *arXiv: 2303.08774*. [Online]. Available: <https://arxiv.org/abs/2303.08774>.
- [29] A. Dosovitskiy, L. Beyer, A. Kolesnikov *et al.*, "An image is worth 16×16 words: Transformers for image recognition at scale," in *Proc. International Conference on Learning Representations (ICLR 2021)*, 2021.
- [30] Z. Wang, A. C. Bovik, H. R. Sheikh, and E. P. Simoncelli, "Image quality assessment: from error visibility to structural similarity," *IEEE transactions on image processing*, vol. 13, no. 4, pp. 600–612, 2004.
- [31] B. Girod, "What's wrong with mean-squared error?" *Digital images and human vision*, pp. 207–220, 1993.
- [32] A. M. Eskicioglu and P. S. Fisher, "Image quality measures and their performance," *IEEE Transactions on communications*, vol. 43, no. 12, pp. 2959–2965, 1995.
- [33] Z. Wang and A. C. Bovik, "A universal image quality index," *IEEE signal processing letters*, vol. 9, no. 3, pp. 81–84, 2002.
- [34] Z. Wang, A. C. Bovik, and L. Lu, "Why is image quality assessment so difficult?" in *2002 IEEE International conference on acoustics, speech, and signal processing*, vol. 4. IEEE, 2002, pp. IV–3313.
- [35] N. Liu and G. Zhai, "Free energy adjusted peak signal to noise ratio (FEA-PSNR) for image quality assessment," *Sensing and Imaging*, vol. 18, pp. 1–10, 2017.
- [36] Z. Wang and A. C. Bovik, "Mean squared error: Love it or leave it? a new look at signal fidelity measures," *IEEE signal processing magazine*, vol. 26, no. 1, pp. 98–117, 2009.
- [37] H. Zhang, Z. Kyaw, S.-F. Chang, and T.-S. Chua, "Visual translation embedding network for visual relation detection," in *Proc. IEEE conference on computer vision and pattern recognition (CVPR)*, 2017, pp. 5532–5540.
- [38] M. Heusel, H. Ramsauer, T. Unterthiner *et al.*, "Gans trained by a two time-scale update rule converge to a local nash equilibrium," *Advances in neural information processing systems (NIPS 2017)*, vol. 30, 2017.
- [39] K. Papineni, S. Roukos, T. Ward, and W.-J. Zhu, "BLEU: A method for automatic evaluation of machine translation," in *Proc. 40th annual meeting of the Association for Computational Linguistics*, 2002, pp. 311–318.
- [40] H. Xie, Z. Qin, G. Y. Li, and B.-H. Juang, "Deep learning enabled semantic communication systems," *IEEE Transactions on Signal Processing*, vol. 69, pp. 2663–2675, 2021.
- [41] J. Devlin, M.-W. Chang, K. Lee, and K. Toutanova, "BERT: Pre-training of deep bidirectional transformers for language understanding," 2018, *arXiv:1810.04805*. [Online]. Available: <https://arxiv.org/abs/1810.04805>.
- [42] J. Johnson, A. Alahi, and L. Fei-Fei, "Perceptual losses for real-time style transfer and super-resolution," in *European conference on computer vision*. Springer, 2016, pp. 694–711.
- [43] J. Wang, Y. Song, T. Leung *et al.*, "Learning fine-grained image similarity with deep ranking," in *Proc. IEEE conference on computer vision and pattern recognition*, 2014, pp. 1386–1393.
- [44] A. Frome, G. S. Corrado, J. Shlens *et al.*, "DeViSE: A deep visual-semantic embedding model," *Advances in neural information processing systems*, vol. 26, pp. 312–321, 2013.
- [45] J. Zhang, Y. Kalantidis, M. Rohrbach *et al.*, "Large-scale visual relationship understanding," in *Proc. AAAI conference on artificial intelligence*, vol. 33, no. 01, 2019, pp. 9185–9194.
- [46] A. Paszke, S. Gross, F. Massa *et al.*, "Pytorch: An imperative style, high-performance deep learning library," *Advances in neural information processing systems*, vol. 32, 2019.
- [47] R. Wightman, "Pytorch image models," 2019. [Online]. Available: <https://github.com/rwightman/pytorch-image-models>.
- [48] G. Cheng, P. Lai, D. Gao, and J. Han, "Class attention network for image recognition," *Sci China Inf Sci*, vol. 66, no. 3, p. 132105, 2023.
- [49] J. Wang, B. Liu, and K. Xu, "Semantic segmentation of high-resolution images," *Sci China Inf Sci*, vol. 60, pp. 1–6, 2017.
- [50] T. Lin, M. Maire, S. J. Belongie *et al.*, "Microsoft COCO: common objects in context," in *Proc. 13th European Conference*, ser. Lecture Notes in Computer Science, vol. 8693. Springer, 2014, pp. 740–755.
- [51] E. Boursoulatte, D. B. Kurka, and D. Gündüz, "Deep joint source-channel coding for wireless image transmission," *IEEE Transactions on Cognitive Communications and Networking*, vol. 5, no. 3, pp. 567–579, 2019.
- [52] D. B. Kurka and D. Gündüz, "Deep joint source-channel coding of images with feedback," in *proc. 2020 IEEE International Conference on Acoustics, Speech and Signal Processing (ICASSP)*, 2020, pp. 5235–5239.
- [53] —, "Bandwidth-agile image transmission with deep joint source-channel coding," *IEEE Transactions on Wireless Communications*, vol. 20, no. 12, pp. 8081–8095, 2021.